

The Failure Analysis of Paralleled Solar Array Regulator for Satellite Power System in Low Earth Orbit

Sung-Soo Jang^{1†}, Sung-Hoon Kim¹, Sang-Ryool Lee¹, and Jaeho Choi²

¹Korea Aerospace Research Institute, Daejeon 305-333, Korea

²Chungbuk National University, Cheongju 361-763, Korea

A satellite power system should generate and supply sufficient electric power to perform the satellite mission successfully during the satellite mission period, and it should be developed to be strong to the failure caused by the severe space environment. A satellite power system must have a high reliability with respect to failure. Since it cannot be repaired after launching, different from a ground system, the failures that may happen in space as well as the effect of the failures on the system should be considered in advance. However, it is difficult to use all the hardware to test the performance of the satellite power system to be developed in order to consider the failure mechanism of the electrical power system. Therefore, it is necessary to develop an accurate model for the main components of a power system and, based on that, to develop an accurate model for the entire power system. Through the power system modeling, the overall effect of failure on the main components of the power system can be considered and the protective design can be devised against the failure. In this study, to analyze the failure mode of the power system and the effects of the failure on the power system, we carried out modeling of the main power system components including the solar array regulator, and constituted the entire power system based on the modeling. Additionally, we investigated the effects of representative failures in the solar array regulator on the power system using the power system model.

Keywords: satellite, electrical power system, space environment, solar array regulator, solar array, battery

1. INTRODUCTION

The low earth orbit (LEO) satellite that is now being developed in Korea requires the power system that is able to supply more electric power and highly reliable in order to obtain high-resolution images and carry out various missions. Since a satellite power system cannot be repaired after launching, different from a ground system, it is necessary to design the system to be robust enough to work normally under various space environments. In satellite where reliability matters greatly, failure mode simulation is very important to verify the performance of a power system. If a power system is tested using the hardware only, the test conditions will be limited because the fabrication of the hardware requires much time and cost,

and the setting up all the surrounding circumstances is difficult. Thus, the test under the conditions similar to those of space environment should be performed using a power system model based on the accurate analysis and modeling of the power system components such as solar array regulator, battery, and solar array. Further, since the protective system can be designed on the basis of the tested system data and the system to which the protective technique has been applied can be tested again, and thus the reliability of the entire system can be elevated.

In this article, the effect of the failure mode on the power system was investigated as regards the power system structure of the LEO satellite that is being developed in Korea, that is, the unregulated bus with 50 V bus power supply, for the failure mode that may take place in the

© This is an Open Access article distributed under the terms of the Creative Commons Attribution Non-Commercial License (<http://creativecommons.org/licenses/by-nc/3.0/>) which permits unrestricted non-commercial use, distribution, and reproduction in any medium, provided the original work is properly cited.

Received Jan 14, 2011 Revised Feb 15, 2011 Accepted Feb 23, 2011

[†]Corresponding Author

E-mail: ssjang@kari.re.kr

Tel: +82-42-860-2389 Fax: +82-42-860-2007

parallel operation of the small-power capacity/high-efficiency solar array regulator. Firstly, we performed modeling of the main components of the power system to investigate the effects of the solar array regulator failure mode on the power system. We realized the modeling of the solar array that is the primary energy source (Rauschenbach 1980), battery that is the secondary energy source (Zimmerman & Peterson 1970, Scott & Rusta 1979), and the solar array regulator that regulates the power provision to the battery and spacecraft loads. Then, a simple power system model of unregulated bus structure with 50 volt bus power supply was constituted using the developed model for the components (Patel 2005).

2. MODELING OF THE POWER SYSTEM COMPONENTS

As shown Fig. 1, the power system in this article has the unregulated bus structure where the satellite bus voltage is directly determined by the battery. The power system consists of the solar array that provides the pri-

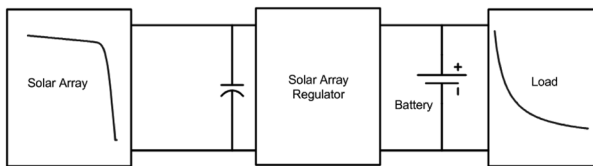


Fig. 1. Electrical power system architecture.

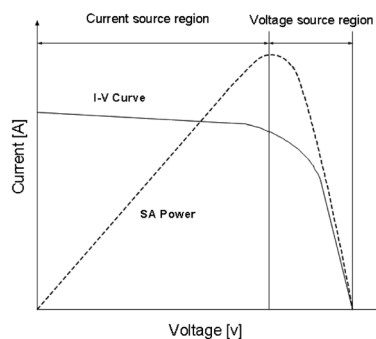


Fig. 2. Solar cell I-V curve.

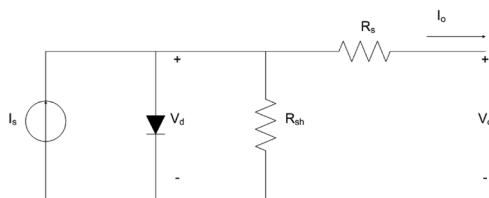


Fig. 3. The equivalent circuit model of solar cell.

mary power for the satellite load and battery recharging during sunlight, the battery that provides power during an eclipse, and the solar array regulator that converts the power generated by the solar array and provides it to the satellite bus. The solar array regulator was designed to use the small-power capacity/high-efficiency solar array regulator modules by connecting them in parallel. The paralleled solar array regulator in which the solar array modules are connected in parallel allows additional parallel connection of the developed small-power capacity/high-efficiency solar array regulator modules for the effect conversion and provision of high power capacity as the power capacity of satellites becomes larger. The followings describe the modeling of the main components that was performed to develop the model for the entire power system.

2.1 Modeling of the Solar Array

The solar array has non-linear output characteristics of negative impedance as shown in Fig. 2. The maximum power point divides the region that shows the current source characteristics and the regions that shows the voltage source characteristics and they show different output patterns depending on the variation of the temperature and the solar radiation amount. As the temperature decreases, the open circuit voltage (Voc) is increased though the short circuit current (Isc) is little changed. As the amount of solar radiation increases, on the contrary, Isc is increased though Voc is little changed. Fig. 3 shows the modeling of the non-linear characteristics of the solar array.

Based on the circuit model of the solar array, the voltage-current equation was derived as shown in Eq. (1) in which the output current can be calculated with given input voltage by the Newton Raphson iteration method. The output variation by the temperature and the solar radiation is expressed as in Eq. (2).

$$I_o = I_s - I_{do} \left[\exp \left(\frac{QV_d}{AKT} \right) - 1 \right] - \frac{V_d}{R_{sh}}$$

$$V_d = V_o + I_o R_s \tag{1}$$

$$\Delta I = f_c \Delta T, \quad \Delta V = (f_v + f_c R_s) \Delta T \tag{2}$$

where, Q = electron charge, K = Boltzmann constant, A = curve fitting constant, f_c = current temp.constant, f_v = voltage temp. constant, ΔT = Ref. (28°C) – current temp.

The solar array is constituted by series and parallel

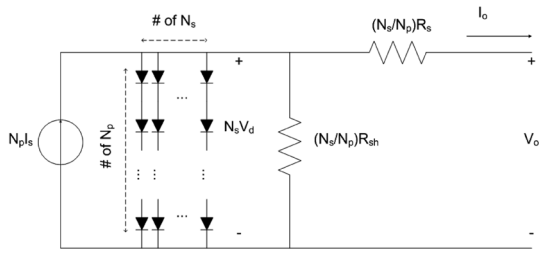


Fig. 4. The equivalent circuit model of solar array.

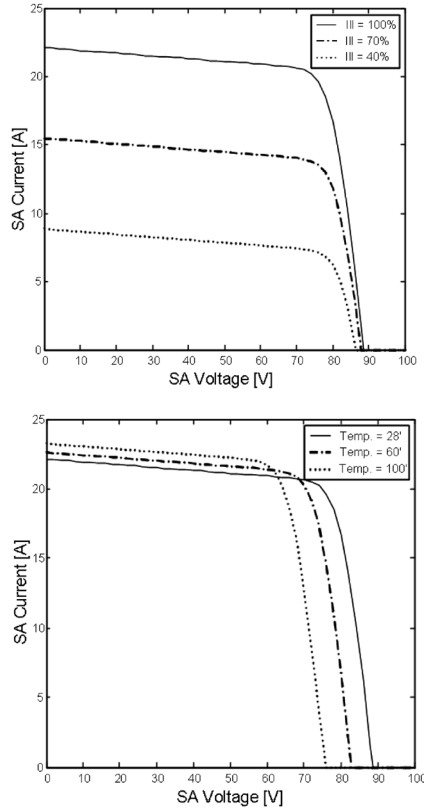


Fig. 5. The simulated I-V curve of solar array w.r.t illumination and temperature.

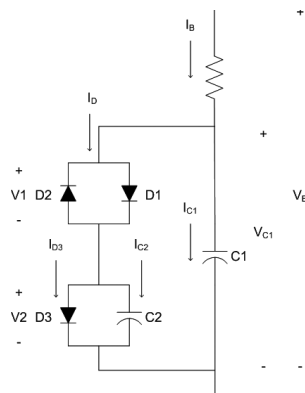


Fig. 6. The equivalent battery model.

connection of solar cells. If the solar array model is built by connection of the solar cell equivalent circuit model, the numerical variations in each device can be applied without change, but too much computer resource is consumed. Thus, the solar array model is built as a single solar cell using macro-technique. Fig. 4 shows the macro-model equivalent circuit of the solar array. Based on the equivalent circuit, the voltage-current equation was derived as Eq. (3):

$$I_o = N_p \left[I_s - I_{do} \left\{ \exp\left(\frac{QV_d}{AKT}\right) - 1 \right\} - \frac{V_d}{R_{sh}} \right]$$

$$V_d = \frac{V_o}{N_s} + \frac{I_o R_s}{N_p} \tag{3}$$

where, N_s = number of the series cell, N_p = number of the parallel cell.

The I_{sc} and V_{oc} of the solar cell model in our study were 0.265 A and 1.0306 V, respectively. The solar array was constituted by connecting 86 solar cells in each string and the entire system is composed of 56 strings. Fig. 5 shows the I-V characteristic curve of the solar cell array model.

2.2 Modeling of the Battery

Since battery is the device to store electric energy, it can be considered as a very large capacitor due to its basic characteristics. However, different from the general linear capacitors, battery shows a very non-linear characteristic because of the chemical reaction of the inner chemical factors. Due to the chemical reactions, battery shows non-linear charge-discharge characteristics, different from the linear characteristics of capacitor. The representative characteristic is the hysteresis phenomenon where the paths of voltage variation are different when charging and discharging. Additionally, while the output voltage is increased without limitation when current flows into the ideal capacitor, the output voltage is not increased but maintains a constant value in a battery when the charging continues beyond the capacity limit. The capacitance of a battery is varied by the output voltage if the input current is constant. Fig. 6 shows the battery model based on the Zimmerman model where the nonlinear characteristics are expressed as the combination of diodes and capacitors. Eq. (4) is the circuit equation to describe the relation between the input current and output current in the battery:

$$\begin{aligned}
 & - D1, D2 \\
 & I_D = 2k_1 \sinh(k_3 V_1) \quad , \quad - C1, C2 \\
 & - D3 \quad \quad \quad C = A \exp[-B(V - V_M)^2] + D \\
 & I_{D3} = k_1 \exp[k_3 V_1 - 1] \quad (4)
 \end{aligned}$$

where,

$$k_1 = \frac{I_o \exp[40.27k_2(1 - \frac{519}{T+459})]}{\exp[40.27\frac{I_o}{T}] - 1}, k_3 = \frac{20900}{L(T+459)}, I_o = \text{reference diode current [A]@60°F and } V_o, V_o = \text{reference diode current [V]@60°F and } I_o, T = \text{actual diode temperature [°F]}, L, k_2 = \text{fitting constant, } C = \text{capacitance [F]@V, } V = \text{actual voltage of capacitor [V], } V_M = \text{median voltage [V], } A = \text{capacitance [F]@V=V_M, } B = \text{distribution constant}$$

Fig. 7 shows the results of the charge-discharge simulation of the nickel-cadmium battery model at 0 and 28°C of which capacitance is 43 AH.

2.3 Modeling of the Solar Array Regulator

The solar array regulator plays the fundamental and important roles of regulating the solar cell power according to the load and battery status. Its main functions of the solar array regulator are performed by the switching of the semiconductor devices. Modeling is required to perform the stress analysis for the stable functioning of the semiconductor devices and the verification of the dynamic characteristics of the regulator.

2.3.1 Modeling of the Passive Device

The Passive devices in the solar array regulator are inductor and capacitor. Eq. (5) is the voltage-current equation of the circuit model that considers the individual parasitic resistances (Erickson & Maksimovie 2001). In

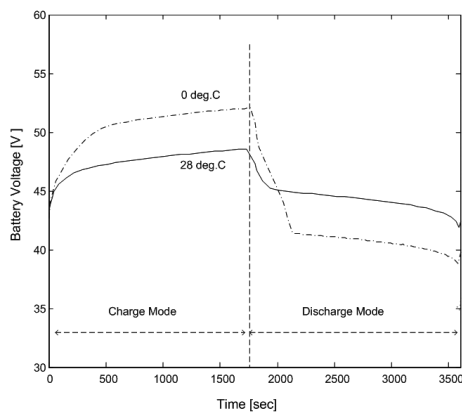


Fig. 7. The simulated battery charging/discharging curve w.r.t temperature.

the model, the inductor is considered as the output current depending on the input voltage, and the capacitor as the output voltage depending on the input current

$$\begin{aligned}
 \text{Inductor: } I &= \frac{1}{L} \int (V - RI) dt \\
 \text{Capacitor: } V &= \frac{1}{C} \int Idt + RI \quad (5)
 \end{aligned}$$

2.3.2 The Switching Network Model

The switching network used for the solar array regulator was the buck topology. In modeling the switching network function, we considered the average model that uses switching duty ratio. In the average model, the output ratios for the two input states are generated in the average model using the duty ratio. Since the average should be made both in the continuous current mode and the discontinuous current mode, the determinants of two modes and the gain ratios in each mode are determined firstly. The switching network can be modeled as the ideal transformer with a gain ratio as shown in Fig. 8. The case where the waveform of the inductor current flowing through the switching network is reduced to zero within the switching period is considered as the discontinuous current mode. The determinants of the continuous/discontinuous current modes and the gain at each mode are calculated as in Eq. (6) using the boundary value between the discontinuous current mode and the continuous current mode with the general buck converter working characteristics. Fig. 9 shows the simulation model for the buck topology regulator realized by using the Simulink switching function.

$$\begin{aligned}
 M &\equiv \frac{V_2}{V_1} = \frac{I_1}{I_2} = \frac{D}{D_A} \\
 D_A &= D + \frac{2LI_2}{DTV_1} = \begin{cases} \geq 1, & \text{CCM } D_A = 1 \\ < 1, & \text{DCM } D_A = D_A \end{cases} \quad (6)
 \end{aligned}$$

2.3.3 Modeling of the Current Controller

The current controller for the parallel operation of the solar array regulator was built to generate switching duty ratio (pulse width modulation) using the inductor current of the solar array regulator. The charge current mode controller, used as the controller in this study, generates the switching duty ratio by integrating the current flowing through the switch when the switch is on and comparing it with the reference control voltage. Fig. 10 shows the relation between the switching current and the charge current in the charge current mode controller.

The switching duty ratio generated by using the relation can be expressed as in Eq. (7):

$$v_A = \frac{1}{C} \int_0^{DT} R_i i_{sw} dt = v_c, \quad \frac{1}{C} R_i I_L DT = v_c, \quad D = \frac{C v_c}{R_i I_L T} \quad (7)$$

3. MODELLING OF THE POWER SYSTEM AND THE ANALYSIS OF THE FAILURE CHARACTERISTICS IN THE PARALLEL SOLAR ARRAY REGULATOR OPERATION MODES

3.1 Modeling of the Power System

Using the model for the main components of the power system described in Section 2, we constituted the power system model of the unregulated bus structure that uses a 50 V bus power supply, as shown in Fig. 11. The design values used for the setting of the model for the solar array regulator and the battery can be freely changed so that the capacity of the power system can be easily expanded depending on the power requirements to perform the satellite mission. Additionally, the small-

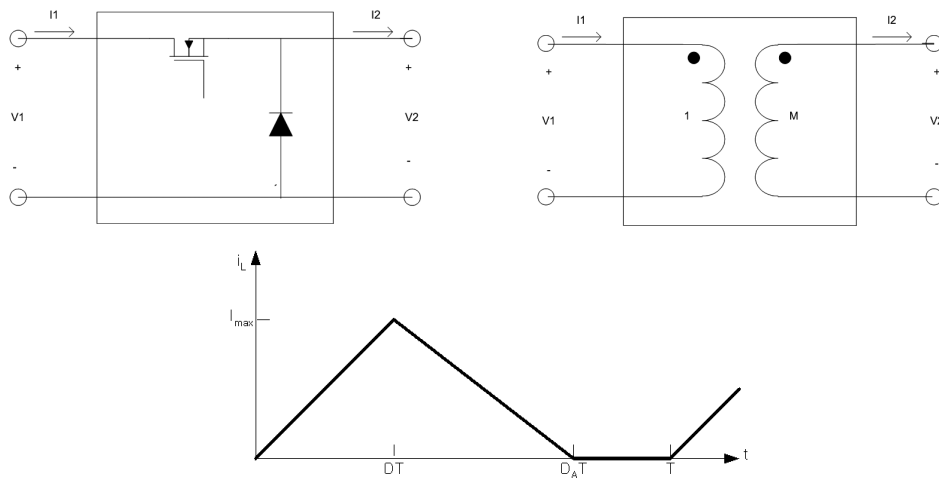


Fig. 8. The switching network and equivalent model of buck converter, and inductor current waveform.

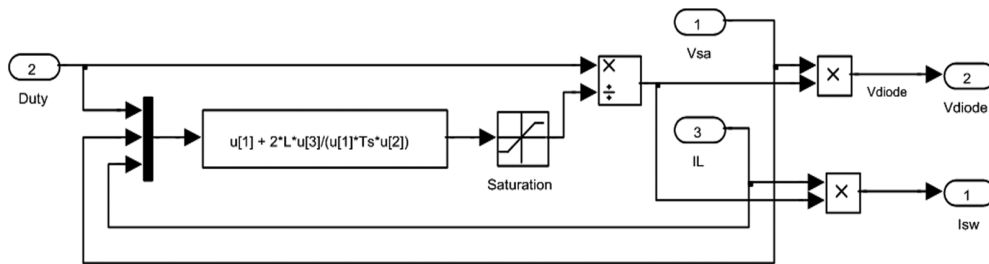


Fig. 9. The simulation model of buck converter controller.

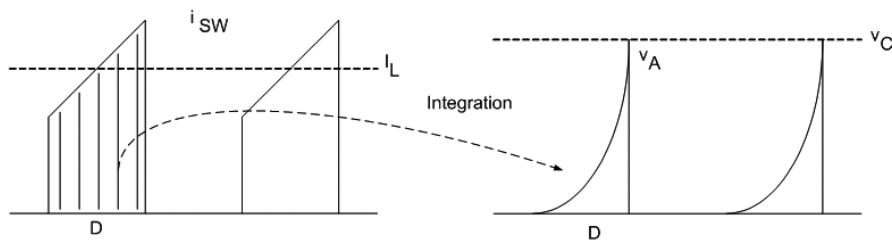


Fig. 10. The operation concepts of switching controller using charge current mode.

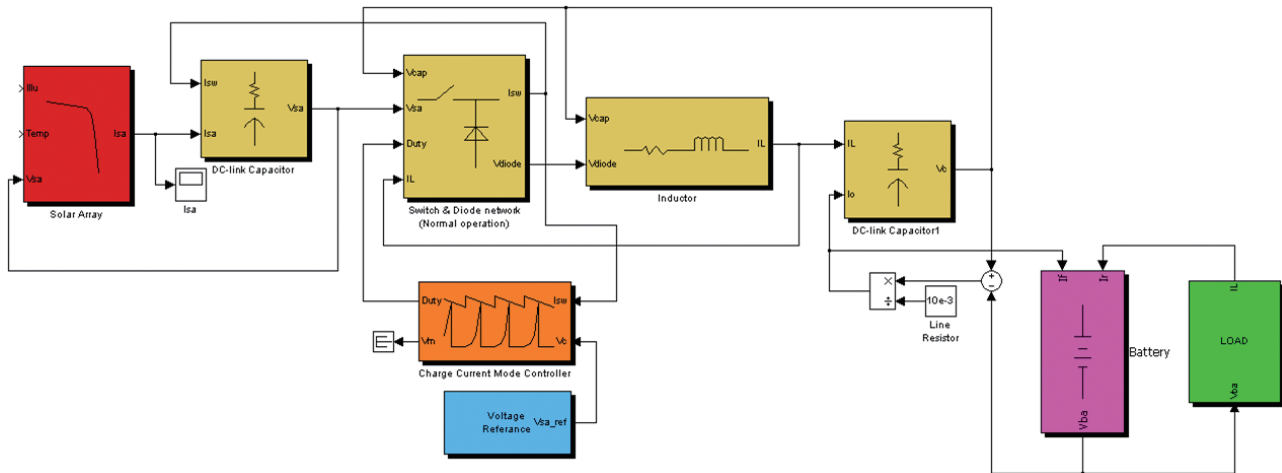


Fig. 11. Electrical power system modeling with 50 V unregulated bus.

capacity/high-efficiency solar array regulator modules can be operated in parallel so that the solar array regulator can be developed effective as the satellite power capacity becomes larger. In this study, the power system was established in the structure where two solar array regulator modules that can convert 500 W are operated in parallel. When the power conversion capacity should be increased in a satellite, small-capacity/high-efficiency solar array regulators can be easily added to establish the power system of a higher capacity. Table 1 lists the design values of the main components considered in the power system model.

3.2 The Analysis of the Operation Mode Failure Characteristics of the Paralleled Solar Power Regulator

We analyzed the effect of the operation mode failure

Table 1. The design parameters in EPS modeling.

Units	Parameters	Values
Solar array	Cell short circuit current (I_{sc})	0.265 A
	Cell open circuit voltage (V_{oc})	1.0306 V
	No. of cells per string (N_s)	86 cells
	No. of strings (N_p)	56 strings
	Nominal temperature	28°C
Battery	Capacity per cell	45 AH
	No. of cells per string	35 cells
	Initial voltage per cells	1.2 V
Solar array Regulator	Inductor	95 μ H
	Switching frequency	100 kHz
DC-link Capacitor	Capacitor	90 μ F
	ESR of inductance	0.1 Ω
Load	Resistor	500 W

EPS: electrical power system, DC, direct current, ESR: equivalent series resistance.

of the parallel modules in the solar array regulator on the power system. Since the modules are connected in parallel in the solar power regulator as the power capacity of the satellite power system is increased, we analyzed the effect of failure in one of the paralleled modules on the other modules. We took into account the short and open failure of the switch and the short failure of the capacitor in the solar array regulator as the failures that may happen during the parallel operation of the solar array regulator considered in this article.

Fig. 12 shows the result of the power system simulation with a short failure of the switch in the solar array regulator module (#2). Once a short failure of the switch takes place in the solar array regulator module (#2), the input voltage of the solar array regulator was dropped down to 20 V temporarily, but the battery voltage was not changed significantly. The inductor current of the solar array regulator module (#2) shows a large pulse at the moment of short switch failure, and the current sharing with the paralleled modules was broken. Using this information, it can be verified that the short failure has taken place at the module where the current is increased. The failed module can be separated by inserting an auxiliary switch in front of the module and turning it off. After the failed module (#2) is separated, the array works normally as the normal module (#1) bears all the power.

Fig. 13 shows the simulation result of the open failure of the switch in the solar array regulator module (#2). Since the module where the open failure of the switch has taken place is separated from the whole system naturally and the normal module bears all the power, the action of the entire system is not significantly affected. As can be seen from the simulation results of the short and

open switch failures in the solar array regulator, the design capacity value should be determined to have a margin sufficient for the normal modules to bear the power of the failed module when a failure occurs in one of the

paralleled module.

Fig. 14 shows the effect of the short failure of the capacitor in solar array regulator module (#2) on the power system. When the short failure of the capacitor takes

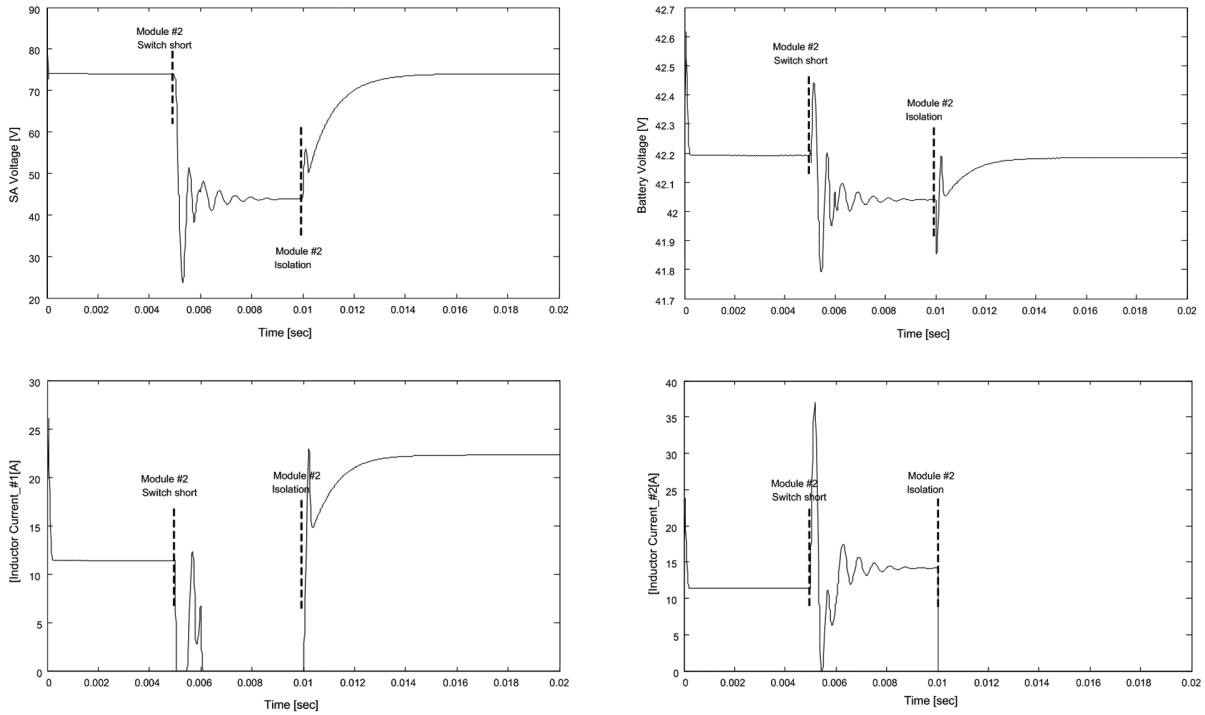


Fig. 12. Electrical power system response during switch short failure in solar array regulator module.

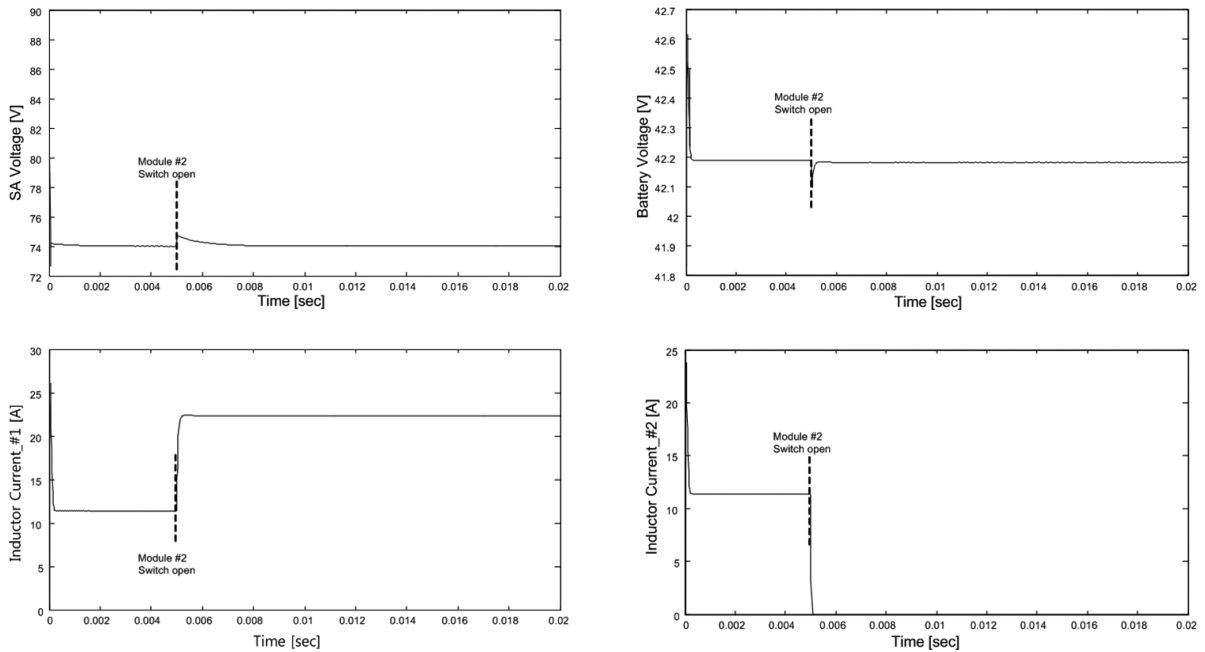


Fig. 13. Electrical power system response during switch open failure in solar array regulator module.

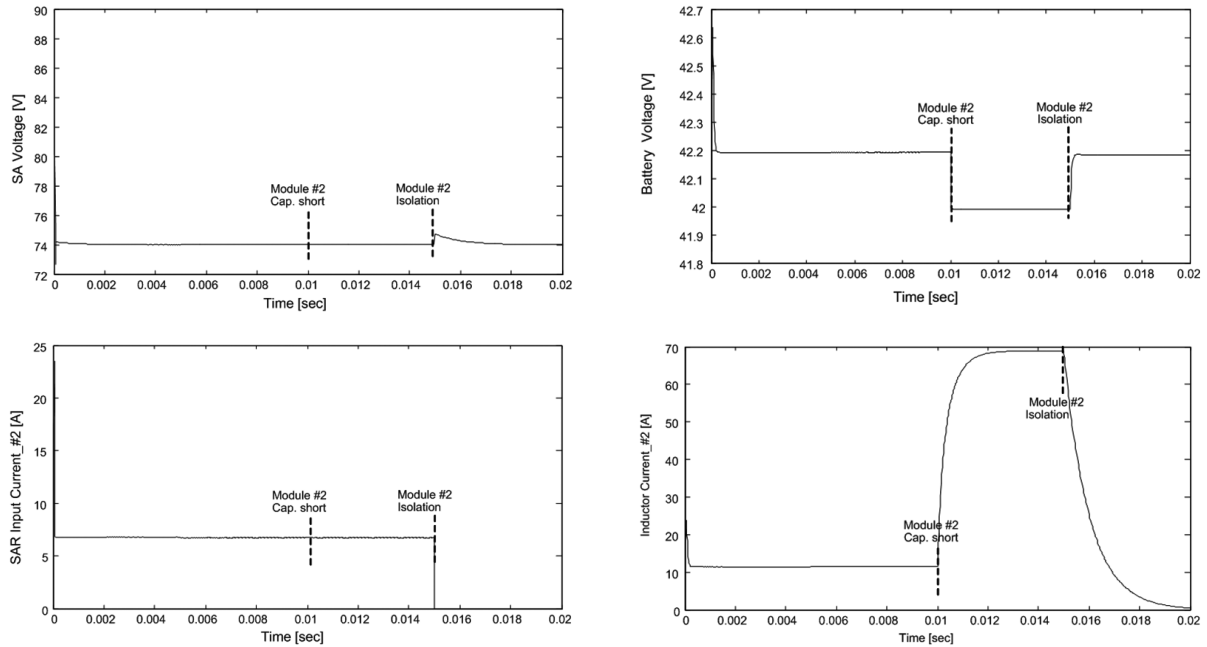


Fig. 14. Electrical power system response during capacitor short failure in solar array regulator module.

place, the output voltage of the solar array regulator was dropped by about 0.2 V, but there was not a significant variation. However, since the controlling was performed, in this study, in the charge current mode where the amount of the switch current integration in the solar array regulator is controlled, the inductor current continued to increase up to 70 A during the switching current integration. Thus, different from the case of a switching failure where only the input current of the solar array regulator needs to be sensed, the inductor current should be sensed additionally in the case of a short failure of the capacitor to detect and separate the failed module.

4. CONCLUSIONS

In this article, we considered the failure modes that can take place during the parallel operation of the small-capacity/high-efficiency solar array regulator in order to meet the requirement of high power capacity that is gradually increasing to perform various satellite missions and obtain high-resolution images. For the effect of the power system failure modes on the system, we performed modeling of the main components of the power system based on the power system of the LEO satellite that is now developed in Korea, and constituted the power system model that has unregulated bus structure. Additionally, we analyzed the power system characteristics

considering the failure modes that can take place during the paralleled operation of the solar array regulator using the established power system model.

To develop a satellite power system that is highly reliable in space environment, it is necessary to analyze the performance of the power system in preparation for the structural changes in the future by supplementing the main components model of the power system. The development of hardware test bed for power system performance analysis is limited because it requires much development time and budget and it is difficult to simulate all the power system failures. Therefore, the overall performance of the system should be sufficiently reviewed by the development of accurate software test bed for the power system.

In order to efficiently develop a highly reliable power system in the future not only for the LEO satellite but also for the planet exploration, various power system failure modes that can take place in the severest space environment should be analyzed in detail, and the protective design should be sufficiently reviewed considering the effects of the failure modes on the system.

REFERENCES

Erickson RW, Maksimovic D, Fundamentals of power electronics, 2nd ed. (Kluwer Academic, Norwell, 2001), 39-56.

Patel MR, Spacecraft power systems (CRC Press, Boca Raton, 2005), 58-131.

Rauschenbach HS, Solar cell array design handbook: the principles and technology of photovoltaic energy conversion (Van Nostrand Reinhold Co., New York, 1980), 30-149.

Scott WR, Rusta DW, Sealed cell nickel cadmium battery ap-

plications manual (National Aeronautics and Space Administration, Washington, DC, 1979), 325-407.

Zimmerman HG, Peterson RG, An electrochemical cell equivalent circuit for storage battery/power system calculations by digital computer, in Proceedings of the 5th International Energy Conversion Engineering Conference, 1970, 6.33-6.39.